ACS APPLIED ELECTRONIC MATERIALS

pubs.acs.org/acsaelm Letter

Centimeter-Sized Monolayer CVD Graphene with High Power Factor for Scalable Thermoelectric Applications

Matthias Schrade,* Wen Xing, Knut Thorshaug, and Branson D. Belle

Cite This: ACS Appl. Electron. Mater. 2022, 4, 1506−1510 Read Online

ACCESS | Metrics & More | Article Recommendations | Supporting Information

ABSTRACT: Among the many extraordinary qualities of graphene, its thermoelectric properties have attracted significant interest, for example, in active cooling applications. Here, we report on the thermoelectric transport properties of centimeter-sized monolayer CVD graphene, electrostatically controlled by a high-capacity ionic gel. The power factor reaches 7 and 5.4 mW m^{-1} K^{-2} for hole and electron conduction, respectively, similar to earlier reports obtained for microdevices despite our devices being over 2 orders of magnitude larger. On the basis of these results, we propose nonvolatile ferroelectric polarization as a scalable technology for graphene-based thermoelectric applications.

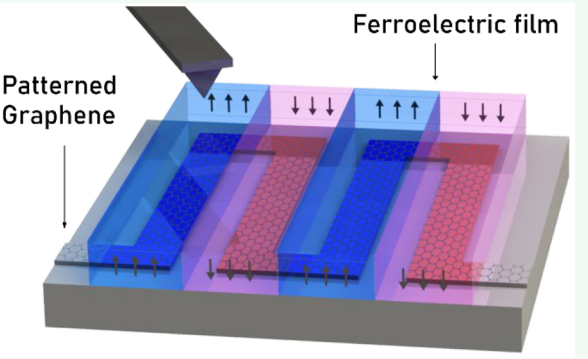

KEYWORDS: *graphene, electrostatic doping, thermoelectric, ionic gel, ferroelectric*

Thermoelectric (TE) energy conversion is a fascinating technology with immense application potential, spanning from industrial waste heat regeneration to on-chip microelectronic cooling.[1] This versatility is further combined with additional advantages including a noiseless operation, low maintenance, scalability, and long lifetime. Nonetheless, thermoelectric devices are today still restricted to niche applications, as available TE materials suffer from various major shortcomings, including a high price, toxicity, and low chemical stability.[2]

During the past decades, much effort has been spent on finding new superior TE materials.[3] The quality of a TE material can be described by its figure-of-merit, $zT = \frac{S^2 T}{\rho\kappa}$, where S is the Seebeck coefficient, ρ the electrical resistivity, κ the thermal conductivity, and T the absolute temperature. The term including the electronic properties of zT is often called the power factor, $PF = S^2/\rho$. All the material properties that contribute to zT are dependent on the charge carrier concentration n of the material, and maximizing zT is therefore a task of precisely manipulating n. For bulk materials, the carrier concentration is usually changed by extrinsic chemical doping, rendering material optimization tedious and resource-intensive, as for each specific carrier concentration, at least one sample needs to be synthesized and characterized.

Control of n can also be achieved via the field effect. Here, an electric field is applied across an insulating dielectric, inducing a conductive layer at the interface. By changing the applied voltage, the carrier concentration of the sample can be conveniently and reversibly changed and the corresponding transport properties studied.[4] As the applied electric field is usually screened within a few nanometers, the applicability of such electrostatic doping is mainly limited to very thin films. By definition, two-dimensional (2D) materials with few atomic layers are ideal for this technique. Consequently, electrostatic doping is routinely used to study the transport properties of various 2D materials.[5] Nonetheless, combining TE measurements with electrostatic doping is less common. Notwithstanding, several experimental reports on the promising TE performance of 2D-based devices can be found in the literature.[6,7] In particular, the TE properties of graphene, as the archetypical 2D material representative, have been studied extensively, not only as a probe to develop a fundamental understanding of its electronic properties[8−10] but also to target practical applications like self-powered sensors.[11,12] Most studies on the TE properties of 2D materials are done on microdevices built by using advanced microtechnological fabrication techniques, while for practical applications, large, homogeneous, and scalable samples are needed, so that the generated energy or cooling power is sufficient. Therefore, in this study, we have characterized the TE properties of large, centimeter-scaled monolayer graphene devices prepared by chemical vapor deposition (CVD). The carrier concentration is

Received: October 11, 2021
Accepted: March 21, 2022
Published: March 23, 2022

varied via electrostatic doping using a high capacitance ionic gel, so that maximum TE performance in both the p- and n-type regime can be reached with only small gate voltages, $V_G \leq 1.75$ V. The obtained power factor (PF) is similar to earlier results on microfabricated devices, and we discuss prospects for practical applications of graphene-based thermoelectrics.

Large 1 × 1 cm^2 field-effect devices have been fabricated by using commercial monolayer CVD on quartz and a drop-casted ionic gel as the gate dielectric. A sketch of the experimental setup is shown in Figure 1a, complemented by representative raw data in Figure 1b,c. Details on the chemicals used and measurement procedure are given in the Supporting Information, section S1.

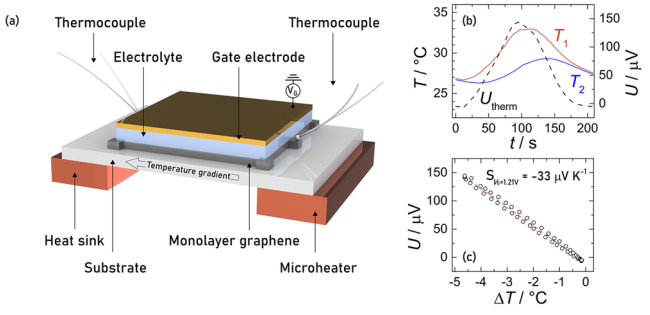

Figure 1. (a) Schematic of the thermoelectric experimental setup. A dielectric gel is drop-casted on a 1 cm^2 large sample of monolayer graphene on quartz and connected with thermocouples and four current electrodes. (b) Raw data of a typical measurement of the Seebeck coefficient. A microheater creates a temperature gradient across the sample, and the corresponding voltage U_{therm} between the thermocouples is recorded simultaneously. (c) The Seebeck coefficient is obtained as a linear fit of the Cu-lead corrected U_{therm} versus $\Delta T = T_2 - T_1$.

The measured sheet resistance, the Seebeck coefficient, the power factor $PF = S^2/\rho$, and the Hall resistance as a function of applied gate voltage V_G are shown in Figure 2. To convert sheet resistance into bulk resistivity ρ, we use a thickness of monolayer graphene of 3.3 Å. Without any applied V_G, the sample has a Seebeck coefficient of +30 μV K^{-1} and a positive Hall resistance, indicating p-type behavior due to adsorbed atmospheric molecules and acceptor-type impurities introduced by the CVD production process.[13] With increasing V_G, the Fermi level rises toward the Dirac point, where the sheet resistance reaches a maximum at V_G = 0.75 V. The ratio between minimum and maximum resistance is $\frac{R_{S,max}}{R_{S,min}} \approx 8$. The resistance maximum is accompanied by a sign change of both Seebeck coefficient and Hall resistance, in agreement with a change from p-type to predominantly n-type conduction at higher V_G. Our measurements show a slight hysteresis upon V_G cycling, in agreement with earlier reports and explained by charge carrier trapping at defects at the graphene−electrolyte and graphene−substrate interfaces.[14] These defect sites are—at least in part—related to the presence of atmospheric humidity, as can be seen from the measurements in controlled atmospheres for a different sample (Figure S2).

The maximum Seebeck coefficient in the p-type region (+68 μV K^{-1}) is larger than the absolute Seebeck value in the n-type region (−58 μV K^{-1}), resulting in a power factor, $PF = S^2/\rho$, which is slightly asymmetric in V_G. The lower Seebeck coefficient for electron charge carriers as compared to holes has been observed earlier and attributed to their different carrier mobility and effective density of states.[8,15]

To discuss the electronic properties in more detail, it is helpful to convert the applied V_G into the sheet carrier concentration n_S as described in section S2 of the Supporting Information. The mobility is then calculated by $\mu = (R_S n_S e)^{-1}$ and shown in Figure 3. The mobility of holes is higher than that of electrons, in our case 800 and 600 cm^2 V^{-1} s^{-1}, respectively, at a hole and electron concentration of 5 × 10^{12} cm^{-2}. These mobility values obtained here are similar to earlier reports for ionically gated CVD graphene,[16] and the higher mobility for holes compared to electrons explains the higher Seebeck coefficient and thus the higher power factor in the p-type region.

With the carrier concentration inferred from the Hall effect measurements, we can also revisit the gating dynamics of our sample. Figure S4 shows the sheet resistance and Seebeck coefficient plotted against the extracted carrier concentration. The small hysteresis visible in the original data with a dynamically changing V_G (Figure 2a−c) has disappeared, indicating that the role of interfacial charge trapping upon gating merely renormalizes the carrier concentration but leaves the overall band structure and carrier scattering unchanged. The maximum PF is obtained for a carrier concentration of 5 × 10^{12} in both the p- and n-type regime.

Comparing the TE properties obtained here with earlier reports, we find that our results for centimeter-scaled, commercial graphene are similar to values reported for devices, which were fabricated by sophisticated microfabrication techniques (Table S1).

Therefore, in this context, we discuss the potential of graphene in TE applications. Its peculiar band structure and extremely high electrical conductivity cause—despite its moderate Seebeck coefficient—a high PF at room temperature, rivaling state-of-the-art thermoelectric materials. For comparison, the PF of the most commercially used TE material Bi_2Te_3 is around 4.5 mW m^{-1} K^{-2}.[17] Notwithstanding, the thermoelectric figure-of-merit of graphene is very low (≈0.0005 at 300 K, using an in-plane thermal conductivity of 4000 W K^{-1} m^{-1} for polycrystalline CVD graphene[18]). However, it has been argued that the PF and not zT is most relevant for many applications as (i) the thermal conduction will be largely dominated by the substrate and gate structure and not the graphene film itself,[15] (ii) the power factor determines the amount of heat, which can be pumped in active cooling applications,[19] and (iii) a large PF maximizes the power output under infinite heat source conditions, often realized for electronic cooling or industrial waste heat.[20]

The high PF of graphene-based thermoelectrics comes with additional advantages like sample transparency, flexibility, and established etching and patterning protocols, making them attractive candidates for various thermoelectric applications.[21] However, a significant obstacle that still exists is the absence of scalable manufacturing routines for large-scale TE devices. For example, Kanahashi et al. have estimated that at least 10^4 p−n couples are needed to power simple Internet-of Things (IoT) devices like sensors from body heat. In stark contrast, experimentally demonstrated devices consist only of a few pairs (<10),[11,22,23] primarily due to the lack of efficient methods to reliably control the charge carrier concentration of graphene. Duan et al. have proposed a graphene-based device, where the p- and n-type regions are electrostatically doped to their maximum PF by lithographically patterned gate

https://doi.org/10.1021/acsaelm.1c00995
ACS Appl. Electron. Mater. 2022, 4, 1506−1510

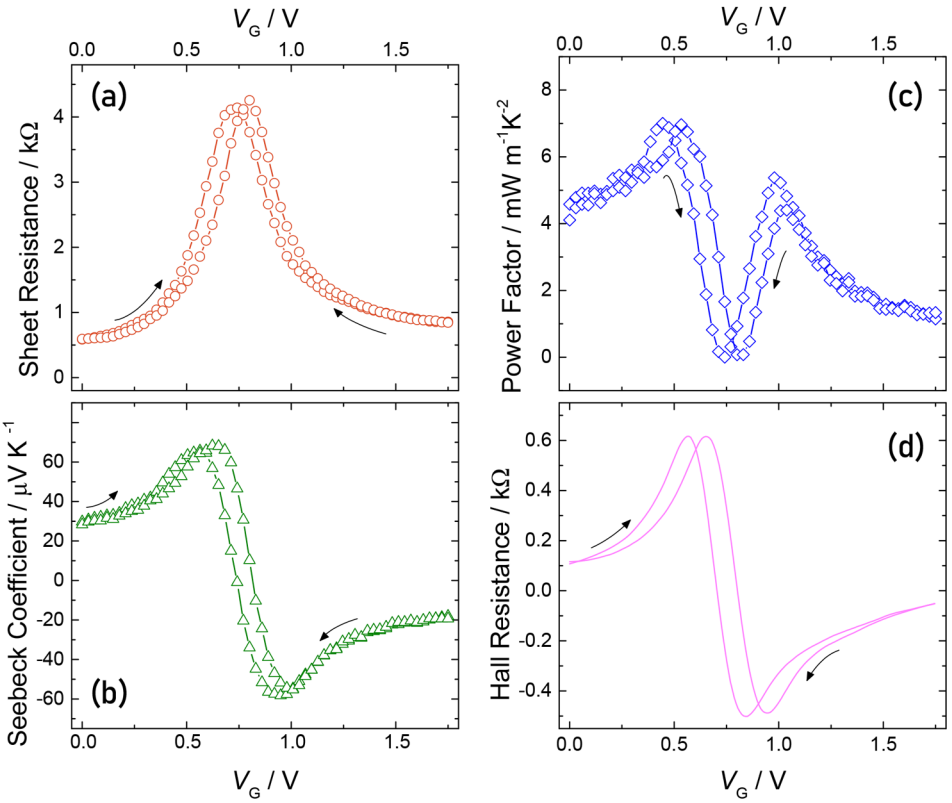

Figure 2. Experimental results for a single device. (a) Sheet resistance R_S, (b) Seebeck coefficient S, (c) power factor $PF = S^2/\rho$, and (d) Hall resistance as a function of applied gate voltage V_G. The sample changes from p- to n-type behavior at the Dirac point around V_G = 0.75 V. The observed hysteresis can be associated with trapped charges at the interface.

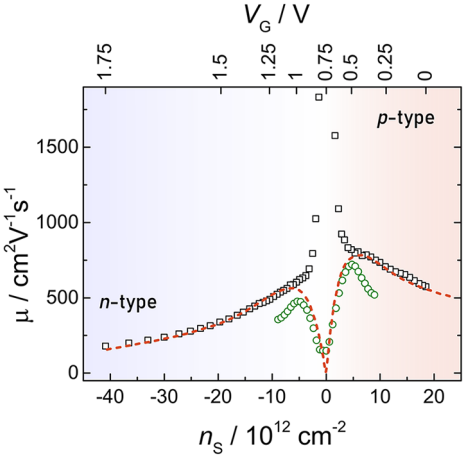

Figure 3. Extracted mobility using the data from Figure 2 as a function of sheet carrier concentration n_S. Black squares are a result from the simple Drude formula $\mu = \sigma/(n_S e)$, valid at large $|n_S|$, while green circles are calculated by differentiating σ_S with respect to n_S, valid at low $|n_S|$. The red dashed line indicates an approximate overall mobility interpolating the two regimes, as discussed in detail in section S2.

structures. They argued that such a structure could be used for the active cooling of hot spots within integrated circuits, where the thermoelectrically pumped heat could enhance the passive cooling effect by at least 10%.[24] However, we believe that the fabrication and integration of a significant number of such gate structures is increasingly complicated. In addition, metallic electrodes would open an unwanted, parallel path for thermal conduction, reducing overall efficiency.

Instead, we here suggest replacing the gate dielectric with a ferroelectric material. It has earlier been shown that the polarization of an adjacent ferroelectric material can electrostatically control the carrier type, concentration, and thus the conductance in graphene in a nonvolatile and reconfigurable way.[25] By moving a biased probe as the gate electrode across the ferroelectric−graphene sample, a polarization pattern can be written into the ferroelectric layer, leading to locally defined regions within the graphene layer with defined carrier type and concentration (Figure 4a).[26] In particular, it is possible to polarize certain regions so that the PF of graphene reaches its maximum value for either p- or n-type conduction.

For example, thin (∼100 nm) layers of the organic ferroelectric poly(vinylidene fluoride-*co*-trifluoroethylene P(VDF−TrFE) can be deposited on large areas by using spin-coating.[27] Their thickness combined with a low thermal conductivity of P(VDF−TrFE)[28] would minimize unwanted heat conduction through the dielectric layer.

To demonstrate the principle, we fabricated a similar device using 1 × 1 cm^2 single-layer graphene on 90 nm SiO_2 with a spin-coated P(VDF−TrFE) film on top. Figure 4b shows the poling characteristics of this device, with a reversible switch in the ferroelectric polarization at ≈±100 V. This high voltage is related to the relative thickness of our film (≈1 μm), and fabrication parameters would need to be optimized to achieve lower switching voltages for practical applications. More importantly, the two polarization directions of the ferroelectric layer correspond to two distinctly different, nonvolatile states of electronic transport in the adjacent graphene layer: The

https://doi.org/10.1021/acsaelm.1c00995
ACS Appl. Electron. Mater. 2022, 4, 1506−1510

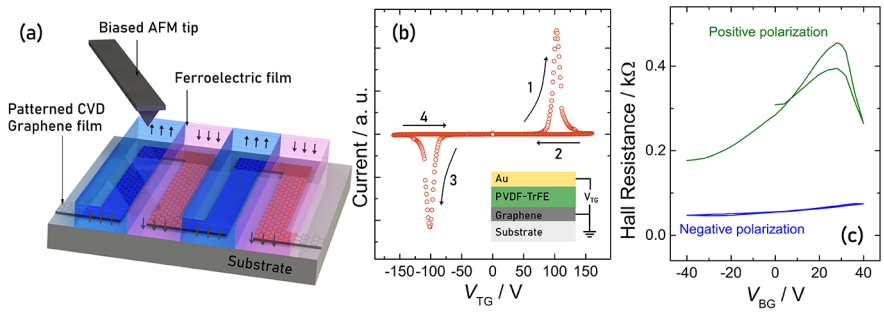

Figure 4. (a) Schematic of the proposed thermoelectric device. A large-scale CVD graphene layer is lithographically patterned into the desired geometry, here forming the conventional, π-shaped design of a TE generator. A deposited ferroelectric layer is then locally polarized by moving a biased probe across the sample, so that specific regions have optimal p- and n-type PF. (b) Poling behavior of a deposited P(VDF−TrFE) film on graphene. At ±100 V, the polarization changes, as detected by a sharp peak in the current. (c) The Hall resistance for the same device in two different polarization states of the ferroelectric layer as a function of V_{BG} applied over the 90 nm SiO_2 back gate. The Hall resistance is significantly higher for positive polarization, reflecting a lower sheet carrier concentration and showing an onset of sign reversal at higher V_{BG}.

sheet resistance changes by more than 400% (Figure S5), also reflected in the Hall resistance, changing from 60 to 290 Ω (Figure 4c), corresponding to a change in n_S from 38×10^{12} to 7×10^{12} cm^{-2}. Unlike earlier reports in the literature,[25,29] the remanent polarization of our P(VDF−TrFE) film was not strong enough to induce a change in the majority carrier type from p- to n-type, although the onset of a p−n transition is visible for the positively polarized state when an additional voltage is applied at the back gate. However, a successful demonstration of the proposed writable TE generator requires further optimization of the VDF/TrFE ratio, deposition parameters, and postdeposition curing temperature.

The advantages of such ferroelectrically controlled TE devices include flexible device proportions, unconventional geometry, small feature size, and reconfigurability. Potential scalability limitations related to the finite writing speed of the moving gate electrode were recently addressed by studies demonstrating the optical control of ferroelectric polarization, so that the required polarization patterns can be rapidly created by illuminating only partial regions of the sample.[30]

In summary, we have characterized the thermoelectric properties of centimeter-sized, macroscopic, single-layer CVD graphene, electrostatically gated by an ionic gel. A large variation of the sheet carrier concentration by 6×10^{13} cm^{-2} was observed by using a gate voltage of only 1.75 V. The simultaneously measured Seebeck coefficient and sheet resistance follow the typical behavior for CVD graphene driven from its as-synthesized p-type state into the n-type region. A large maximum power factor of 7 and 5.4 mW K^{-2} m^{-1} respectively for hole and electron conduction is observed at room temperature, similar to values obtained for microscopic devices fabricated from exfoliated graphene. We propose doping by ferroelectric polarization as a viable means for scalable fabrication of efficient nanoscale devices for on-chip cooling purposes and demonstrate a ferroelectrically controlled, nonvolatile, and reversible change in resistivity by more than 400%.

■ ASSOCIATED CONTENT

Supporting Information

The Supporting Information is available free of charge at https://pubs.acs.org/doi/10.1021/acsaelm.1c00995.

Experimental details; literature comparison of obtained power factor; impact of measurement atmosphere on gating hysteresis; discussion on the determination of carrier density and associated mobility; transport properties vs n_S; resistivity hysteresis for ferroelectrically controlled sample (PDF)

■ AUTHOR INFORMATION

Corresponding Author

Matthias Schrade − *Department of Sustainable Energy Technology, SINTEF Industry, 0373 Oslo, Norway;* orcid.org/0000-0002-9501-6536; Email: matthias.schrade@sintef.no

Authors

Wen Xing − *Department of Sustainable Energy Technology, SINTEF Industry, 0373 Oslo, Norway*

Knut Thorshaug − *Department of Process Technology, SINTEF Industry, 0373 Oslo, Norway;* orcid.org/0000-0002-3797-5448

Branson D. Belle − *Department of Sustainable Energy Technology, SINTEF Industry, 0373 Oslo, Norway;* orcid.org/0000-0002-1211-8714

Complete contact information is available at: https://pubs.acs.org/10.1021/acsaelm.1c00995

Notes

The authors declare no competing financial interest.

■ ACKNOWLEDGMENTS

M.S. is thankful for Dean Hasall at ATC Semitec with the microheaters used to create the temperature gradients and Ole Bjørn Karlsen from the University of Oslo practical help with the electrode deposition. Financial support from the research council of Norway through the Allotherm project (314778) and SINTEF is gratefully acknowledged.

■ REFERENCES

(1) Snyder, G. J.; Toberer, E. S. Complex thermoelectric materials. *Nat. Mater.* **2008**, *7*, 105−114.

(2) He, R.; Schierning, G.; Nielsch, K. Thermoelectric Devices: A Review of Devices, Architectures, and Contact Optimization. *Adv. Mater. Technol.* **2018**, *3*, 1700256.

(3) He, J.; Tritt, T. M. Advances in thermoelectric materials research: Looking back and moving forward. *Science* **2017**, *357*, eaak9997.

(4) Ahn, C. H.; Bhattacharya, A.; Di Ventra, M.; Eckstein, J. N.; Frisbie, C. D.; Gershenson, M. E.; Goldman, A. M.; Inoue, I. H.;

Mannhart, J.; Millis, A. J.; Morpurgo, A. F.; Natelson, D.; Triscone, J.-M. Electrostatic modification of novel materials. *Rev. Mod. Phys.* **2006**, *78*, 1185−1212.
(5) Chhowalla, M.; Jena, D.; Zhang, H. Two-dimensional semiconductors for transistors. *Nat. Rev. Mater.* **2016**, *1*, 16052.
(6) Lee, M.-J.; Ahn, J.-H.; Sung, J. H.; Heo, H.; Jeon, S. G.; Lee, W.; Song, J. Y.; Hong, K.-H.; Choi, B.; Lee, S.-H.; Jo, M.-H. Thermoelectric materials by using two-dimensional materials with negative correlation between electrical and thermal conductivity. *Nat. Commun.* **2016**, *7*, 12011.
(7) Kanahashi, K.; Pu, J.; Takenobu, T. 2D Materials for Large-Area Flexible Thermoelectric Devices. *Adv. Energy Mater.* **2020**, *10*, 1902842.
(8) Zuev, Y. M.; Chang, W.; Kim, P. Thermoelectric and Magnetothermoelectric Transport Measurements of Graphene. *Phys. Rev. Lett.* **2009**, *102*, 096807.
(9) Wei, P.; Bao, W.; Pu, Y.; Lau, C. N.; Shi, J. Anomalous Thermoelectric Transport of Dirac Particles in Graphene. *Phys. Rev. Lett.* **2009**, *102*, 166808.
(10) Vera-Marun, I. J.; van den Berg, J. J.; Dejene, F. K.; van Wees, B. J. Direct electronic measurement of Peltier cooling and heating in graphene. *Nat. Commun.* **2016**, *7*, 11525.
(11) Zeng, W.; Tao, X.-M.; Lin, S.; Lee, C.; Shi, D.; Lam, K.-h.; Huang, B.; Wang, Q.; Zhao, Y. Defect-engineered reduced graphene oxide sheets with high electric conductivity and controlled thermal conductivity for soft and flexible wearable thermoelectric generators. *Nano Energy* **2018**, *54*, 163−174.
(12) Zhang, D.; Zhang, K.; Wang, Y.; Wang, Y.; Yang, Y. Thermoelectric effect induced electricity in stretchable graphene-polymer nanocomposites for ultrasensitive self-powered strain sensor system. *Nano Energy* **2019**, *56*, 25−32.
(13) Wei, P.; Liu, N.; Lee, H. R.; Adijanto, E.; Ci, L.; Naab, B. D.; Zhong, J. Q.; Park, J.; Chen, W.; Cui, Y.; Bao, Z. Tuning the Dirac Point in CVD-Grown Graphene through Solution Processed n-Type Doping with 2-(2-Methoxyphenyl)-1,3-dimethyl-2,3-dihydro-1H-benzoimidazole. *Nano Lett.* **2013**, *13*, 1890−1897.
(14) Lee, Y. G.; Kang, C. G.; Jung, U. J.; Kim, J. J.; Hwang, H. J.; Chung, H.-J.; Seo, S.; Choi, R.; Lee, B. H. Fast transient charging at the graphene/SiO_2 interface causing hysteretic device characteristics. *Appl. Phys. Lett.* **2011**, *98*, 183508.
(15) Kanahashi, K.; Ishihara, M.; Hasegawa, M.; Ohta, H.; Takenobu, T. Giant power factors in p- and n-type large-area graphene films on a flexible plastic substrate. *npj 2D Materials and Applications* **2019**, *3*, 44.
(16) Lim, G.; Kihm, K. D.; Kim, H. G.; Lee, W.; Lee, W.; Pyun, K. R.; Cheon, S.; Lee, P.; Min, J. Y.; Ko, S. H. Enhanced Thermoelectric Conversion Efficiency of CVD Graphene with Reduced Grain Sizes. *Nanomaterials* **2018**, *8*, 557.
(17) Cha, J.; Zhou, C.; Cho, S.-P.; Park, S. H.; Chung, I. Ultrahigh Power Factor and Electron Mobility in n-Type $Bi_2Te_{3-x}Cu_x$ Stabilized under Excess Te Condition. *ACS Appl. Mater. Interfaces* **2019**, *11*, 30999−31008.
(18) Lee, W.; Kihm, K. D.; Kim, H. G.; Shin, S.; Lee, C.; Park, J. S.; Cheon, S.; Kwon, O. M.; Lim, G.; Lee, W. In-Plane Thermal Conductivity of Polycrystalline Chemical Vapor Deposition Graphene with Controlled Grain Sizes. *Nano Lett.* **2017**, *17*, 2361−2366.
(19) Zebarjadi, M. Electronic cooling using thermoelectric devices. *Appl. Phys. Lett.* **2015**, *106*, 203506.
(20) Narducci, D. Do we really need high thermoelectric figures of merit? A critical appraisal to the power conversion efficiency of thermoelectric materials. *Appl. Phys. Lett.* **2011**, *99*, 102104.
(21) Zong, P.-A.; Liang, J.; Zhang, P.; Wan, C.; Wang, Y.; Koumoto, K. Graphene-Based Thermoelectrics. *ACS Appl. Energy Mater.* **2020**, *3*, 2224−2239.
(22) Novak, T. G.; Kim, J.; Kim, J.; Tiwari, A. P.; Shin, H.; Song, J. Y.; Jeon, S. Complementary n-Type and p-Type Graphene Films for High Power Factor Thermoelectric Generators. *Adv. Funct. Mater.* **2020**, *30*, 2001760.
(23) Lin, Y.; Liu, J.; Wang, X.; Xu, J.; Liu, P.; Nie, G.; Liu, C.; Jiang, F. An integral p-n connected all-graphene fiber boosting wearable thermoelectric energy harvesting. *Compos. Commun.* **2019**, *16*, 79−83.
(24) Duan, J.; Wang, X.; Lai, X.; Li, G.; Watanabe, K.; Taniguchi, T.; Zebarjadi, M.; Andrei, E. Y. High thermoelectricpower factor in graphene/hBN devices. *P. Natl. Acad. USA* **2016**, *113*, 14272.
(25) Zheng, Y.; Ni, G.-X.; Toh, C.-T.; Tan, C.-Y.; Yao, K.; Özyilmaz, B. Graphene Field-Effect Transistors with Ferroelectric Gating. *Phys. Rev. Lett.* **2010**, *105*, 166602.
(26) Wu, G.; Tian, B.; Liu, L.; Lv, W.; Wu, S.; Wang, X.; Chen, Y.; Li, J.; Wang, Z.; Wu, S.; Shen, H.; Lin, T.; Zhou, P.; Liu, Q.; Duan, C.; Zhang, S.; Meng, X.; Wu, S.; Hu, W.; Wang, X.; Chu, J.; Wang, J. Programmable transition metal dichalcogenide homojunctions controlled by nonvolatile ferroelectric domains. *Nat. Electron.* **2020**, *3*, 43−50.
(27) Pi, Z.; Zhang, J.; Wen, C.; Zhang, Z.-b.; Wu, D. Flexible piezoelectric nanogenerator made of poly(vinylidenefluoride-co-trifluoroethylene) (PVDF-TrFE) thin film. *Nano Energy* **2014**, *7*, 33−41.
(28) Zhao, J.; Tan, A. C.; Green, P. F. Thermally induced chain orientation for improved thermal conductivity of P(VDF-TrFE) thin films. *J. Mater. Chem. C* **2017**, *5*, 10834−10838.
(29) Chen, Y.; Zhou, Y.; Zhuge, F.; Tian, B.; Yan, M.; Li, Y.; He, Y.; Miao, X. S. Graphene−ferroelectric transistors as complementary synapses for supervised learning in spiking neural network. *npj 2D Materials and Applications* **2019**, *3*, 31.
(30) Li, T.; Lipatov, A.; Lu, H.; Lee, H.; Lee, J.-W.; Torun, E.; Wirtz, L.; Eom, C.-B.; Íñiguez, J.; Sinitskii, A.; Gruverman, A. Optical control of polarization in ferroelectric heterostructures. *Nat. Commun.* **2018**, *9*, 3344.

https://doi.org/10.1021/acsaelm.1c00995
ACS Appl. Electron. Mater. 2022, 4, 1506−1510